Neural Networks 22 (2009) 30–40

Contents lists available at ScienceDirect

Neural Networks

journal homepage: www.elsevier.com/locate/neunet

Impact of network topology on decision-making☆

Suojun Lu [a], Jian'an Fang [a], Aike Guo [b], Yueqing Peng [b,*]

[a] College of Information Science & Technology, Donghua University, 2999 North Renmin Road, Songjiang District, Shanghai 201620, China

[b] Institute of Neuroscience, Shanghai Institutes for Biological Sciences, Chinese Academy of Sciences, 320 Yueyang Road, Shanghai 200031, China

ARTICLE INFO

Article history:
Received 3 August 2007
Received in revised form
17 September 2008
Accepted 30 September 2008

Keywords:
Complex network
Small-world
Scale-free
Decision-making
Recurrent model

ABSTRACT

The dynamical behaviors of a neural system are strongly influenced by its network structure. The present study investigated how the network structure influences decision-making behaviors in the brain. We considered a recurrent network model with four different topologies, namely, regular, random, small-world and scale-free. We found that the small-world network has the best performance in decision-making for low noise, whereas the random network is most robust when noise is strong. The four networks also exhibit different behaviors in the case of neuronal damage. The performances of the regular and the small-world networks are severely degraded in distributed damage, but not in clustered damage. The random and the scale-free networks are, on the other hand, quite robust to both types of damage. Furthermore, the small-world network has the best performance in strong distributed damage.

© 2008 Elsevier Ltd. All rights reserved.

1. Introduction

Decision-making is a fundamental cognitive behavior in the daily life of animals and humans (for reviews, see Ganguli et al. (2008), Glimcher (2003), Schall (2001), Platt (2002), Smith and Ratcliff (2004), and Sugrue, Corrado, and Newsome (2005)). A large volume of experimental studies has been devoted to understanding the neural basis of decision-making. For instance, in a visual motion discrimination task, monkeys were trained to make a judgment about the direction of motion in a near-threshold stochastic random dot display and report the perceived direction with a saccadic eye movement (Newsome, Britten, & Movshon, 1989). Electrophysiological recording as well as functional brain imaging was carried out to link animal behaviors to neural activities in specific brain areas (Britten, Shadlen, Newsome, & Movshon, 1993; Glimcher, 2003; Newsome et al., 1989; Parker & Newsome, 1998; Platt, 2002; Roitman & Shadlen, 2002; Romo & Salinas, 2001, 2003; Shadlen & Newsome, 1996, 2001). Based on experimental data, a number of computational models were developed to interpret or ascertain the decision-making process in the brain (Bogacz, 2007; Bogacz, Brown, Moehlis, Holmes, & Cohen, 2006; Ditterich, 2006; Machens, Romo, & Brody, 2005; Mazurek, Roitman, Ditterich, & Shadlen, 2003; Usher & McClelland, 2001; Wang, 2002; Wong & Wang, 2006).

A recurrent network model shows that slow synaptic reverberation as well as winner-take-all competition can generate attractor dynamics that reproduces both neurophysiological and psychophysical data (Wang, 2002). Considering the network architecture in this model, each neuron receives input from all other neurons, and the "Hebbian" rule has been used to generate the synaptic weights. So far, however, no theoretical work has explored the potential impact of network topology on decision-making. A study on complex networks has revealed that the architecture of a network can significantly influence its dynamical behavior (for reviews, see Albert and Barabasi (2002), Boccaletti, Latora, Moreno, Chavez, and Hwang (2006) and Newman (2003)). The topology of a biological network often lies between being completely regular and being completely random. To study how the network topology may affect decision-making, we will consider two types of structures, namely, the small-world and the scale-free networks. The concept of small-world networks was proposed by Watts and Strogatz (1998), which captures the fact that many network systems are highly clustered, like regular lattices, yet have small characteristic path lengths, like random graphs. They found that a small-world network displays enhanced signal-propagation speed, computational power, and synchronizing ability. The concept of scale-free networks was proposed by Barabasi and Albert (1999), which encompasses those networks in which the distribution of the connectivity of nodes satisfies the power law. It is found that the scale-free network has even smaller path length than the random network, although it does not show a highly clustered characteristic when the number of nodes is large (Albert & Barabasi, 2002). All these topological properties may affect the dynamical behavior of the network and hence influence the computational process.

☆ Contributed article.

* Corresponding author. Tel.: +86 21 54921787; fax: +86 21 54921735.
E-mail address: yqpeng@ion.ac.cn (Y. Peng).

0893-6080/$ – see front matter © 2008 Elsevier Ltd. All rights reserved.
doi:10.1016/j.neunet.2008.09.012

By constructing a recurrent network model, here we investigated the impacts of network topologies on the alternative decision-making process. We found that the regular and small-world networks have better performance than the other two when the internal noise is low. On the other hand, the random network displays the best performance in the case of strong noise. Their performances are further distinguished when neuronal damages are included. Our results showed that the small-world network displays the best performance in decision-making after neuronal damage, especially for distributed damage.

2. The model and its topological connectivity

We used a recurrent network model (Amit & Brunel, 1997; Wang, 2002) with two competing neural groups ($N = 1000$ for each group; for parameters, see Table 1) to simulate the process of decision-making in a visual motion discrimination task (Fig. 1). Each neuron receives excitatory inputs from neurons in the same group and inhibitory inputs from neurons in the other group. Four different topologies are used to construct the architecture of each group, generating, respectively, the regular, random, small-world and scale-free networks. For the regular network, each neuron is adjacently connected to $k/2$ ($k = 20$) leftward neurons and $k/2$ rightward neurons to form a circuit loop. For the random network, each neuron is randomly connected to other neurons with the total connectivity of $20N$. Then the average degree is:

$$k = 20N/N, \quad \text{then } k = 20.$$

For the small-world network, neuronal connections are modified from the regular network described above with the method of Watts and Strogatz (1998), i.e., parts of regular connections (10%) are randomly reconnected to keep the final average connectivity constant. For the scale-free network, neuronal connections are constructed with the method of Barabasi and Albert (1999). The network starts with a small number of nodes ($m_0 = 30$) and initial edges (random connections, $k_0 = 600$). Then each of new nodes is added by preferentially connecting to the m previous nodes ($m = 20$), according to probability Π:

$$\Pi(k_i) = \frac{k_i}{\sum_{j=1}^{n} k_j} \tag{1}$$

where k_i is the current degree of node i. After T time steps ($T = 970$), we generated a network with N nodes and k average degrees:

$$N = T + m_0, \quad \text{then } N = 1000;$$
$$k = (mT + k_0)/N, \quad \text{then } k = 20.$$

All connections mentioned above are unidirectional. Therefore, the average degree (k) can be divided into inward degrees (k_{in}) and outward degree (k_{out}). Taken together, the four different networks each have the same number of nodes and the same average connectivity. The statistical results of network topology are shown in Table 2.

We denoted I_i as the total synaptic input current to the ith neuron, whose dynamics is given by

$$\tau_{sy}\frac{dI_i}{dt} = -I_i + \alpha\sum_{j=1}^{n} w_{ij}R(I_j) - \beta G\left(\sum_{j=1}^{n} R(I_j)\right) + I_{aff} + I_{bk} \tag{2}$$

where τ_{sy} is the time constant ($\tau_{sy} = 50$ ms), w_{ij} the strength of the synaptic connection from neuron j to i ($w_{ij} = 0$ or 1), $R(I_j)$ the firing rate of neuron j, G the inhibition contribution from the alternative neural group, I_{aff} the afferent input (or external stimuli), and I_{bk} the internal noise. α and β are constants ($\alpha = 25$, $\beta = 20$).

Table 1
Range of model parameters.

Parameters	Description	Value
N	Neuron number within each group	1000
k_{in}	Inward degree of nodes	20
k_{out}	Outward degree of nodes	20
T_{total}	Running Time for each trial (ms)	1000
dt	Integration time step (ms)	0.4
p_{st}	Proportion of stimulated neurons	0.3
μ_0	Basal level of stimuli (mA)	0.2
c'	Coherence level of stimuli	Variable
θ_{exc}	Threshold for neuron firing (mA)	0.6
θ_{max}	Upper threshold for firing rate (mA)	6
θ_{out}	Firing threshold to generate behavior (Hz)	15
τ_{sy}	Time constant of synapse (ms)	50
d_{sy}	Delay time of synaptic transmission (ms)	4
α	Constant of synaptic activity	25
β	Constant of synaptic activity	20
γ	Constant of firing rate	20
ε	Constant of the inhibition strength	0.02
τ_{ns}	Time constant of noise (ms)	5
σ	Noise strength	Variable
P_{dam}	Proportion of damaged neurons	Variable

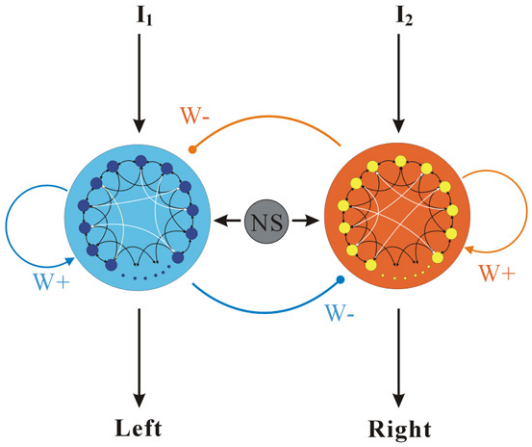

Fig. 1. Schematic depiction of model architecture in decision-making. Two neural groups, each of which is sensitive to one of the two stimuli (I_1 and I_2, mimicking the motion to left or to right, respectively), compete with each other through self-recurrent ($w+$) and mutual inhibition ($w-$). In addition, Gaussian distributed noise (NS) was introduced to the networks to mimic spontaneous neuronal activities (as the internal noise). Inside the neural groups, neurons are connected with each other in different topologies to form four types of network: regular, random, small-world, and scale-free. Here the scheme only shows the small-world network (black links for regular connection, white links for random connection).

Table 2
Statistics of topological features in four networks: inward degree (k_{in}), outward degree (k_{out}), clustering coefficient (cc), and path length (pl).

Network	k_{in}	k_{out}	cc	pl
Regular	20	20	0.711	25.475
Random	20	20	0.040	2.639
Small-world	20	20	0.484	3.214
Scale-free	20	20	0.118	2.563

The firing rate of a neuron (Durstewitz, Seamans, & Sejnowski, 2000) is assumed to be:

$$R(I_i) = \begin{cases} 0 & \text{if } I_i < \theta_{\text{exc}} \\ \gamma \ln(I_i/\theta_{\text{exc}}) & \text{if } \theta_{\text{exc}} \le I_i < \theta_{\text{max}} \\ \gamma \ln(\theta_{\text{max}}/\theta_{\text{exc}}) & \text{if } I_i \ge \theta_{\text{max}} \end{cases} \tag{3}$$

where θ_{exc} is the threshold for neuronal firing ($\theta_{\text{exc}} = 0.6$ mA). The firing rate R saturates when the input reaches the upper threshold θ_{max} ($\theta_{\text{max}} = 6.0$ mA). γ is a constant ($\gamma = 20$ Hz). In parts of computational simulation, we also used a logistic function to

express the firing rate:

$$R(I_i) = Y_{\max} - \frac{Y_{\max}}{1 + \left(\frac{I_i}{\theta_0}\right)^p} \tag{4}$$

where $Y_{\max} = 46$ Hz, to balance the maximum value of the previous firing rate function; $\theta_0 = 2$ mA, $p = 3$.

The inhibition function G is assumed to be a linear function:

$$G(x) = \varepsilon x \tag{5}$$

where ε represents the inhibition strength ($\varepsilon = 0.02$). The synaptic transmission is simulated with a constant delay ($d_{sy} = 4$ ms). Internal noise I_{bk} is introduced to mimic the spontaneous activities of neurons, which satisfies the following equation:

$$\frac{dI_{bk}}{dt} = -\frac{1}{\tau_{ns}}(I_{bk} - I0) + \sigma n(t) \tag{6}$$

where τ_{ns} is the time constant ($\tau_{ns} = 5$ ms), and I_0 the initial state of the total synaptic current ($I_0 = 0.1$ mA). $n(t)$ represents white-noise with zero mean and unit variance, and σ is the noise strength. For most of the simulations, we used $\sigma = 0.5$. To examine the effects of noise on network behavior, we varied σ from 0.5 to 1.0.

3. Results

In this section, we reported the results of our investigation: Section 3.1 examines the effects of network topology on decision-making performance, Section 3.2 studies the noise-resisting capacity of different networks, and Section 3.3 explores the robustness of decision-making subject to neuronal damage.

3.1. Network topology affects decision-making

After a short delay period (200 ms), two stimuli μ_A and μ_B were delivered to the parts of two neural groups ($p_{st} = 30\%$) respectively with a duration of 800 ms, during which two competing neural groups generated the decision-making process. To mimic the visual motion discrimination task in the monkey experiment, we followed the assumption that the output firing rates of the MT cells are linearly proportional to the presented motion coherence (the percentage of randomly moving dots moving in the same direction) (Britten et al., 1993):

$$\begin{cases} \mu_A = \mu_0(1 + c') \\ \mu_B = \mu_0(1 - c') \end{cases} \tag{7}$$

where μ_0 is the base level of the stimuli ($\mu_0 = 0.2$ mA). At the low coherence (small c'), the stimuli to the two neural groups are similar and hard to distinguish. However, the competition between these two neural groups may eventually lead to one of the two attractor states, in which one neural group displays elevated excitatory activity while the other group's activity is suppressed. Suppose that neural group A receives stronger stimuli μ_A, while neural group B receives weaker stimuli μ_B. For instance, in a trial at the coherence level of 0.1, neural group A in the regular network generates excitatory firing by inhibiting the activity of neural group B (Fig. 2a, b). However, the random network fails to generate a winner-take-all pattern, by exhibiting a fluctuation of small neuronal activities in both neural groups (Fig. 2c, d). Similarly, the small-world network also generates robust decision-making process (Fig. 2e, f), while the scale-free network fails (Fig. 2g, h).

To quantify network behaviors, we used the percentage of correct choices (or accuracy) and reaction time as two criteria. A choice is considered as a "correct" action if one neural group receiving a higher external stimulus generates excitatory activity across a certain firing threshold θ_{out}($\theta_{\text{out}} = 15$ Hz). The time point across the threshold is defined as the reaction time. Therefore, a high accuracy or short reaction time indicates good decision-making performance. As shown in Fig. 3, following the increased coherence level, the accuracy (Fig. 3a) for all networks increased while the reaction times (Fig. 3b) decreased. Moreover, we found that the regular and the small-world networks show the highest accuracy among the four networks in a wide range of coherence levels. The scale-free network shows medium accuracy, while the random network displays the worst performance. With respect to reaction time, the small-world network shows the best performance, while the random network still shows the worst performance. The regular and the scale-free networks display a medium reaction time. Considering both accuracy and reaction time, the small-world network offers the best performance in decision-making.

In the above model, we simplified neuronal dynamics by applying a logarithmic function (Eq. (3)) between the firing rate and synaptic current. Then, a hard threshold was set for that firing rate function. The threshold may result in some side-effects, especially in the case of noise inputs. Therefore, we also used a logistic function (Eq. (4)) to exclude the possible effects of the hard threshold on network performance. We found that the four networks show decision-making performances similar to those of the previous model with the threshold logarithmic function (Fig. 4). That is, the regular and the small-world networks show the best performance, while the random network shows the worst performance (Fig. 4c, d). The scale-free network shows a medium performance. This result illustrates that our findings may be not sensitive to the specific firing rate functions.

3.2. Network topology regulates noise-resisting capacity

The biological decision-making process might not be entirely reliable due to noise in the sensory system or in the environment. As mentioned previously, we introduced internal noise to mimic neuronal spontaneous activities, which may be activated by stochastic background inputs inside the brain, rather than external stimuli. However, it is difficult to determine the appropriate amplitude of the noise, which responds to the physiological state of real neurons. Thus, here we examined the effects of internal noise on network behaviors by systematically varying the noise strength σ from 0.5 to 1.0. As shown in Fig. 5, neural networks show spontaneous decision-making even when there was a lack of external stimuli, which is considered as incorrect choices, with high internal noise ($\sigma \geq 0.7$). The incorrect choice percentage became more negative with increasing σ. Finally, all networks make completely incorrect choices at a noise level $\sigma = 1.0$. Further comparison of network behaviors shows that the random network has the best capacity to resist internal noise in a wide range (from $\sigma = 0.7$ to 0.9), while the scale-free network shows the worst performance of noise-resistant capacity. The regular and the small-world networks have similar medium noise-resisting capacity (Fig. 5).

To further investigate the effects of internal noise on the decision-making process, we compared the network behaviors in the presence of both external stimuli and high internal noise. As shown in Fig. 6a, the random network shows the best performance of correct choice in high noise conditions ($\sigma = 0.7$) instead of the worst performance in low noise conditions ($\sigma = 0.5$; Fig. 3). This dramatic change in network behavior further confirms the good noise-resisting capacity of the random network. The other three networks show similar performances of correct choice. However, the random network still shows the worst performance in terms of reaction time (Fig. 6b). In addition, the scale-free network shows the shortest reaction time among all networks.

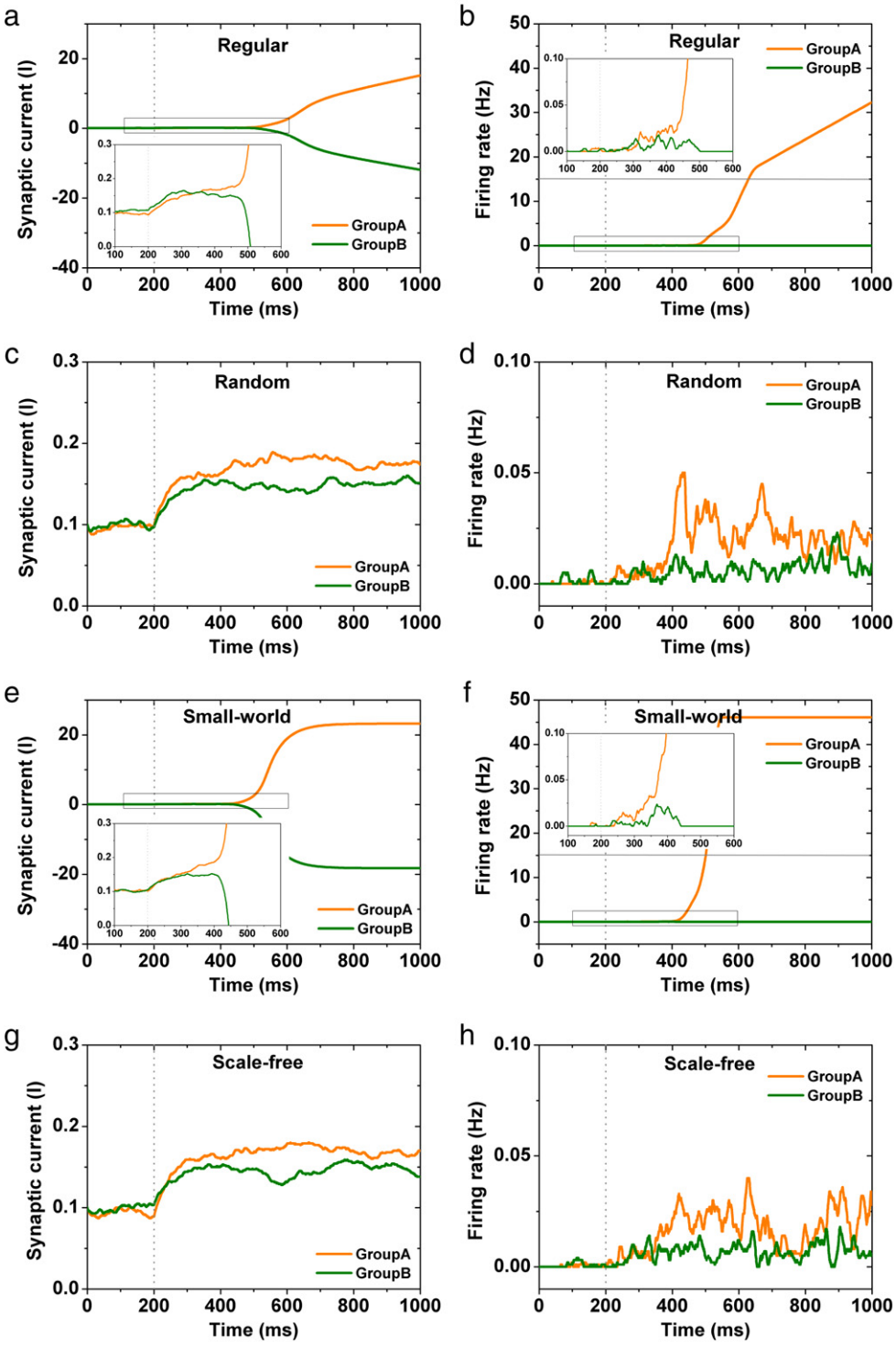

Fig. 2. Samples of individual trials in decision-making at the coherence level of 0.1. a, b. An individual trial of decision-making process in the regular network. The synaptic currents (a) and the firing rates (b) of the neural groups are illustrated. c, d. An individual trial of the decision-making process in the random network. e, f. An individual trial of the decision-making process in the small-world network. g, h. An individual trial of the decision-making process in the scale-free network. Neural group A is supposed to receive stronger stimuli, while neural group B receives weaker stimuli. The decision-making process is simulated in the low internal noise ($\sigma = 0.5$). The insets are enlarged parts of the corresponding boxed regions. The dotted lines indicate the onset of the stimuli. The gray lines indicate the firing threshold to generate decision-making behavior. All curves are the averaged data within the neural group ($N = 1000$).

3.3. Decision-making under neuronal damages

The robustness of network behaviors is a very important criterion of any given network. Many complex systems display a surprising degree of tolerance for errors (Albert & Barabasi, 2002; Albert, Jeong, & Barabasi, 2000). For example, the removal of some nodes has only a weak impact on the network behaviors. The nervous system may be damaged by some physical or biological processes, such as mechanical neural injury or neurodegenerative disease. Here we mimicked these neuronal damages to examine network tolerance during the decision-making process in different topological networks. Due to the

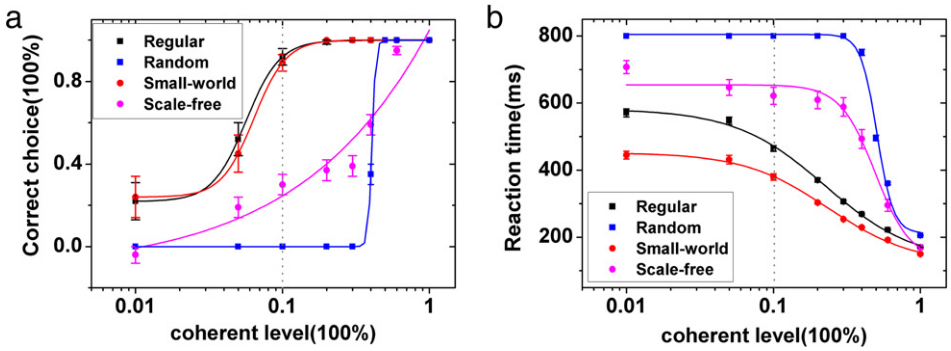

Fig. 3. Effects of network topology on decision-making. a, b. The regular and the small-world networks show significantly higher accuracy and shorter reaction time than other two networks. The decision-making process is simulated in the low internal noise ($\sigma = 0.5$). Data are fitted by the logistic curve ($R^2 > 0.99$ for black, blue, and red curves; $R^2 = 0.94$ and $R^2 = 0.98$ for magenta curves in a and b respectively). For each test point, the data are obtained after an average of 100 trials. The error bar indicates the mean standard error (SEM). (For interpretation of the references to colour in this figure legend, the reader is referred to the web version of this article.)

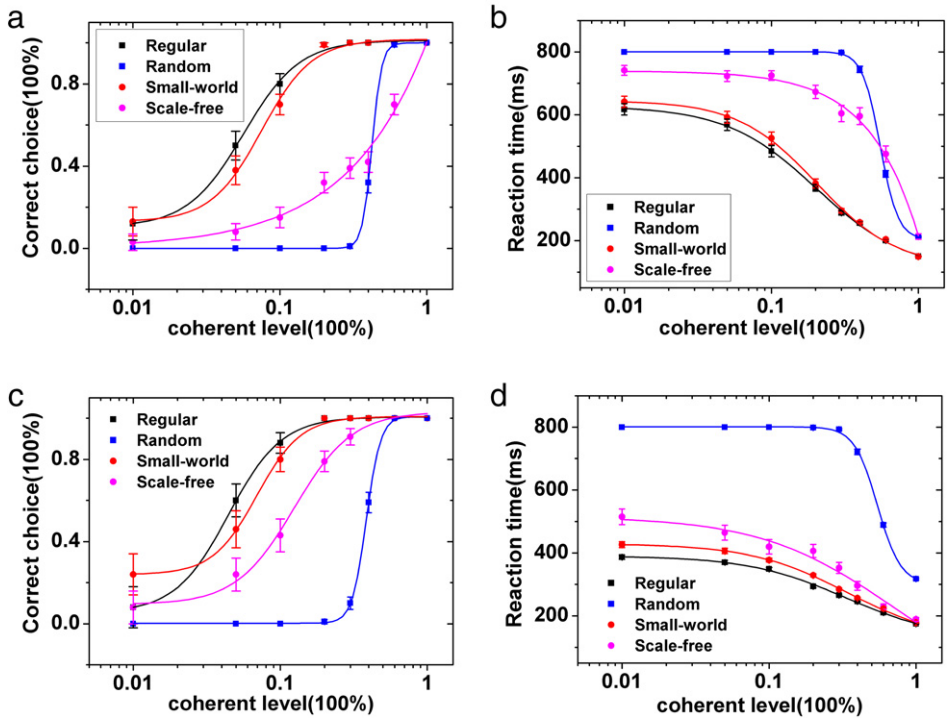

Fig. 4. Effects of firing rate functions on network behaviors. a, b. Decision-making process in the case of a threshold logarithmic function. Here, we reduced the number of neurons in each neural group ($N = 200$). Consequently, the free parameter of the inhibition strength was modified ($\varepsilon = 0.1$). Other parameters remained as shown in the Table 1. c, d. Decision-making process in the case of a logistic function. The modified parameters are: $N = 200$, $\mu_0 = 0.15$, $\varepsilon = 0.1$. Data are fitted by the logistic curve ($R^2 > 0.99$ for all curves except $R^2 = 0.97$ for the magenta curve in d). For each test point, the data are obtained after an average of 100 trials. The error bar indicates the SEM. (For interpretation of the references to colour in this figure legend, the reader is referred to the web version of this article.)

difference in network architecture, different damage patterns may have different effects on decision-making. Therefore, we introduced two kinds of damage patterns: the clustered and the distributed damage patterns. The clustered damage pattern refers to the damage of adjacent neurons from i to $i+x$, where x indicates the number of damaged neurons. The distributed damage pattern refers to random damage to neurons inside a neural group.

We first examined the effects of clustered damage on network behaviors. As shown in Fig. 7a, the regular network shows similar accuracy at different levels of clustered neuronal damage. The reaction time of the regular network in the lower coherence levels slightly decreased under the neuronal damage situation (Fig. 7b). On the contrary, the random network shows a gradual decrease in accuracy under the damage percentage (P_{dam}) from 0 to 0.6 (Fig. 7c). In addition, the reaction time of the random network also gradually increased, following the increase of P_{dam} (Fig. 7d). Similar to the regular network, the small-world network shows no change in accuracy (Fig. 7e) and a slight increase in reaction time (Fig. 7f), following an increase of P_{dam}. Finally, the scale-free network shows a gradually damaged decision-making process in terms of both accuracy and reaction time, following an increase of P_{dam} (Fig. 7g, h). A comparison of network behaviors including both accuracy and reaction time shows that the regular and the small-world networks have significantly better decision-making performance than other two networks at the damage level $P_{\text{dam}} = 0.6$ (Fig. 8).

Then, we examined the effects of distributed damage on network behaviors. Unlike with the clustered damage, both accuracy and reaction time in the regular network are significantly affected by the distributed damage, especially in the high levels of P_{dam} (Fig. 9a, b). At the damage level $P_{\text{dam}} = 0.2$, the regular network shows a similar accuracy to the intact network. The random network still shows a gradual decrease in accuracy and

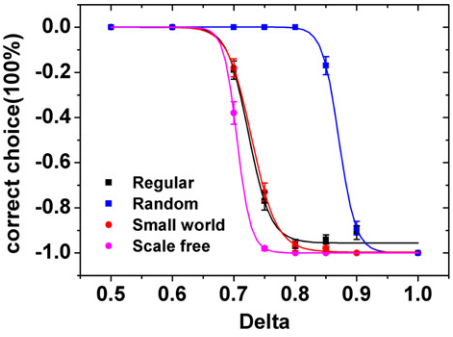

Fig. 5. Effects of network topology on the resistance to internal noise. In high levels of internal noise, the networks generate spontaneous decision-making behavior even without external stimuli, which choices are considered as being incorrect. The random network shows the best capacity to resist internal noise, while the scale-free network shows the worst capacity. Data are fitted by the logistic curve ($R^2 > 0.99$ for all curves). For each test point, the data are obtained after an average of 100 trials. The error bar indicates the SEM.

a gradual increase in reaction times when P_{dam} varies from 0 to 0.6 (Fig. 9c, d). The small-world network shows changes in decision-making similar to those in the regular network (Fig. 9e, f). Finally, the scale-free network also shows gradual changes in both accuracy and reaction time (Fig. 9g, h). At a damage level $P_{\text{dam}} = 0.6$, the small-world network shows the highest accuracy and the shortest reaction times, especially at high coherence levels. The random network shows the worst performance in decision-making (Fig. 10). The regular and the scale-free networks show a medium performance in terms of both accuracy and reaction time. These results indicate that the small-world network has the best capacity to resist distributed neuronal damage.

The above changes in network behaviors may be due to the corresponding changes in network topology in the case of neuronal damage. Therefore, we calculated the topological features of the networks. As shown in Table 3, the regular network shows different changes in topological features between the two different neuronal damage patterns, especially inward and outward degrees. In the distributed damage pattern, the degrees of the regular network are significantly reduced. These reduced degrees lead to a decrease in recruitment of more neurons in the alternative competition, which consequently results in a decrease in decision-making performance. However, in the clustered damage pattern, the degrees are slightly decreased. The random network shows similar changes in topological features in both damage patterns (Table 4). In the small-world network, two types of neuronal damage also induce different changes in topological features (Table 5). That is, the distributed damage pattern causes more severe decrease in network behaviors than the clustered damage pattern. However, the changes are quantitatively different between the two networks. In the case of clustered damage $P_{\text{dam}} = 0.6$, the regular network shows a decision-making performance similar to that of the small-world (Fig. 8). However, in the case of distributed damage $P_{\text{dam}} = 0.6$, the small-world network shows significantly better performance than the regular network in terms of both accuracy and reaction time (Fig. 10). These results indicate that the small-world network has a better capacity to resist neuronal damage, especially distributed damage. Finally, the scale-free network shows similar changes in topological features with both damage patterns (Table 6). Considering the results of network behaviors, these results indicate strong correlations between the changes in network behaviors and the changes in topological features.

4. Discussion

In the present study, we constructed a recurrent network model to simulate the decision-making process. Compared with the previous recurrent model of decision-making (Wang, 2002), here we simplified the dynamical process of neuronal firing by ignoring the detailed descriptions of synaptic currents, such as currents mediated by AMPA, NMDA, and GABA receptors. In such cases, the simulation data, such as reaction time and firing rate, may not exactly mirror the physiological data from the animal study (Roitman & Shadlen, 2002; Shadlen & Newsome, 2001). However, we focused our study on the effects of network topology on decision-making performance by constructing four different types of networks: regular, random, small-world, and scale-free. We found that the regular and the small-world networks show better decision-making performance in the low internal noise situation. However, in the high internal noise situation, the random network shows better decision-making performance. In the case of neuronal damage, especially largely distributed neuronal damage, the small-world network retains the best capacity to execute the decision-making process. All these results indicate that the small-world network exhibits relatively stable network behaviors in decision-making.

Considering the network architecture, previously we constructed the small-world network with 90% regular connection and 10% random connection. To further investigate the effects of network topology on network behaviors, we systematically varied the percentages of random connection from 0% to 100%. Note that the network with 0% random connection is equal to the regular network, while the network with 100% random connection is the random network. Following the percentage increase of random connections, decision-making performances in terms of both accuracy and

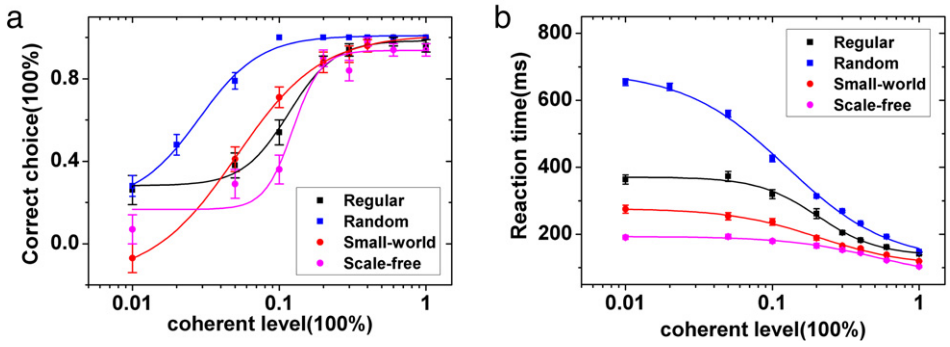

Fig. 6. Effects of network topology on decision-making performance with high internal noise ($\sigma = 0.7$). a. With respect to accuracy, the random network shows the best performance, while the three other networks show similar performance with some fluctuation. b. With respect to reaction time, the random network shows the worst performance, while the scale-free network shows the best performance. Data are fitted by the logistic curve ($R^2 > 0.99$ for all curves except $R^2 = 0.96$ for the magenta curve in a). For each test point, the data are obtained after an average of 200 trials for low coherence levels ($c' \leq 0.1$), and 100 trials for high coherence levels ($c' > 0.1$). The error bar indicates the SEM. (For interpretation of the references to colour in this figure legend, the reader is referred to the web version of this article.)

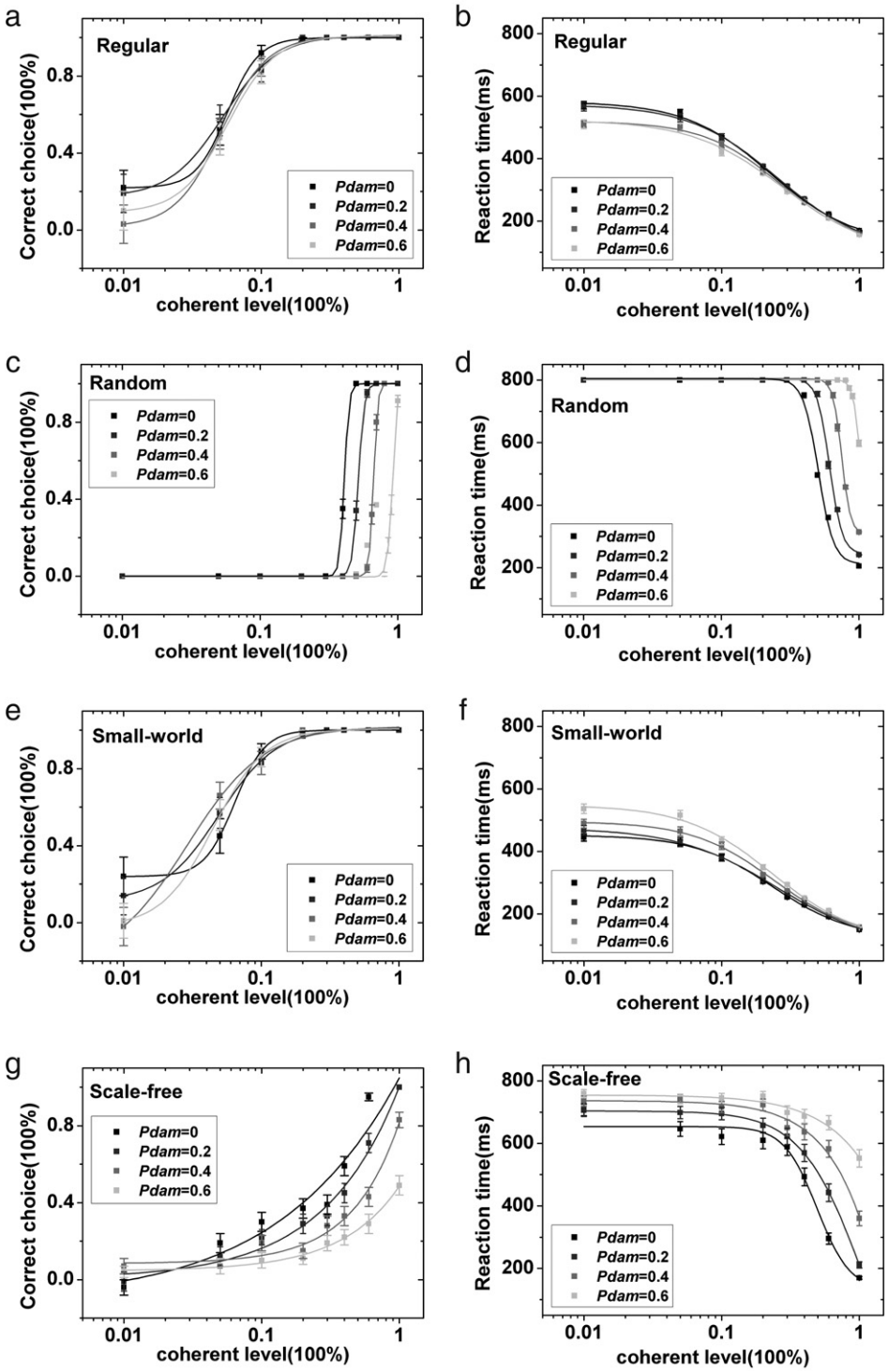

Fig. 7. Effects of network topology on decision-making performance subject to clustered neuronal damage. a, b. The regular network shows similar accuracy and slightly increased reaction time, following a gradual increase of neuronal damage (P_{dam}). c, d. The random network shows a gradual decrease in accuracy and a gradual increase in reaction time with an increase of P_{dam}. e, f. The small-world network also shows similar decrease in accuracy and slight increase in reaction time with an increase of P_{dam}. g, h. The scale-free network shows a gradual decrease in accuracy and gradual increase in reaction time with an increase of P_{dam}.Data are fitted by the logistic curve ($R^2 > 0.99$ for all curves in a–f; $R^2 > 0.94$ for all curves in g, h). For each test point, the data are obtained after an average of 100 trials. The error bar indicates the SEM.

reaction time gradually diminished, especially at high levels of random connections (Fig. 11). However, the networks with low levels of random components (i.e., 10% and 20%) show decision-making performances similar to that of the regular network.

Due to the network architecture, the small-world network contains both regular and random components. Given this, what topological properties contribute to better performance of decision-making in the small-world network, compared with the regular and the random networks? In a recurrent network model, the essential factor in winning a competition between alternative choices is to rapidly recruit activated neurons to exceed the firing threshold (Mazurek et al., 2003; Schall, 2001). Due to the large clustering coefficient in the regular or the small-world networks (Table 2), the recruitment in these networks is more

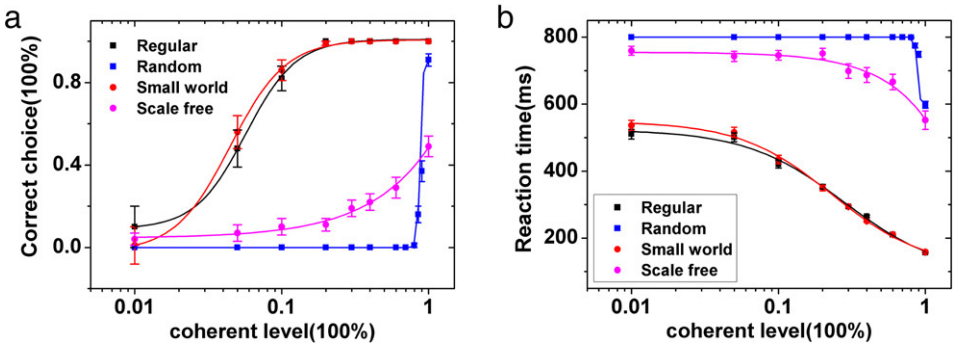

Fig. 8. Comparison of network behaviors at the clustered damage P_{dam} of 0.6. The regular and the small-world networks show significantly better performance in terms of both accuracy (a) and reaction time (b). The decision-making process is simulated in the low internal noise ($\sigma = 0.5$). Data are fitted by the logistic curve ($R^2 > 0.99$ for all curves except $R^2 = 0.97$ for the magenta curve in (b)). For each test point, the data are obtained after an average of 100 trials. The error bar indicates the SEM. (For interpretation of the references to colour in this figure legend, the reader is referred to the web version of this article.)

Table 3
Topological features of the regular network under the conditions of neuronal damages. NaN indicates nonsense data because of some infinite values.

P_{dam}	Distributed damage pattern				Clustered damage pattern			
	k_{in}	k_{out}	cc	pl	k_{in}	k_{out}	cc	pl
0	20	20	0.711	25.475	20	20	0.711	25.475
0.2	15.997	15.997	0.711	26.081	19.863	19.863	0.715	27.152
0.4	11.967	11.967	0.709	27.47	19.817	19.817	0.716	20.486
0.6	8.028	8.028	0.709	NaN	19.725	19.725	0.719	13.821

Table 4
Topological features of the random network under the conditions of neuronal damage.

P_{dam}	Distributed damage pattern				Clustered damage pattern			
	k_{in}	k_{out}	cc	pl	k_{in}	k_{out}	cc	pl
0	20	20	0.04	2.639	20	20	0.04	2.639
0.2	15.977	15.977	0.04	2.708	15.974	15.974	0.04	2.708
0.4	12.012	12.012	0.04	2.829	11.977	11.977	0.039	2.832
0.6	8.012	8.012	0.04	NaN	7.993	7.993	0.039	NaN

Table 5
Topological features of the small-world network under the conditions of neuronal damage.

P_{dam}	Distributed damage pattern				Clustered damage pattern			
	k_{in}	k_{out}	cc	pl	k_{in}	k_{out}	cc	pl
0	20	20	0.484	3.215	20	20	0.484	3.215
0.2	15.99	15.99	0.483	3.402	19.476	19.476	0.522	3.227
0.4	11.983	11.983	0.484	3.717	19.03	19.03	0.564	3.228
0.6	8.008	8.008	0.481	4.358	18.552	18.552	0.61	3.209

Table 6
Topological features of the scale-free network under the conditions of neuronal damage. NaN indicates nonsense data because of some infinite values.

P_{dam}	Distributed damage pattern				Clustered damage pattern			
	k_{in}	k_{out}	cc	pl	k_{in}	k_{out}	cc	pl
0	20	20	0.118	2.563	20	20	0.118	2.563
0.2	16.17	16.17	0.122	2.62	15.954	15.954	0.12	NaN
0.4	12.032	12.032	0.118	NaN	12.049	12.049	0.11	NaN
0.6	8.122	8.122	0.122	NaN	8.112	8.112	0.083	NaN

efficient than that in the random network. Consequently, the regular and the small-world networks have significantly higher accuracy and shorter reaction time than those in the random network in the low internal noise situation. Thus, these results imply that the clustering coefficient may be the key topological parameter in controlling network behaviors in decision-making when the internal noise is low. However, high internal noise leads to large variations in neuronal firing rates. Then, the large clustering coefficient in the regular or the small-world networks may also enlarge the error signals of those variations, which results in a less accurate output of decision-making. On the other hand, the short path length in the random network may contribute to a rapid dispersal of error signals. Therefore, the regular and the small-world networks show lower accuracy than that in the random network when the internal noise is high. However, large clustering coefficients still contribute to the rapid recruitment of competing signals, regardless of whether these signals are efficient signals or error signals when the firing rates are lower than the threshold. Thus, the regular and the small-world networks still show significantly shorter reaction time than that in the random network, especially for low coherence levels. When the neuronal activities in the stimulated cluster exceed the firing threshold, the essential factor in winning the competition is to recruit more neurons from outside that cluster.

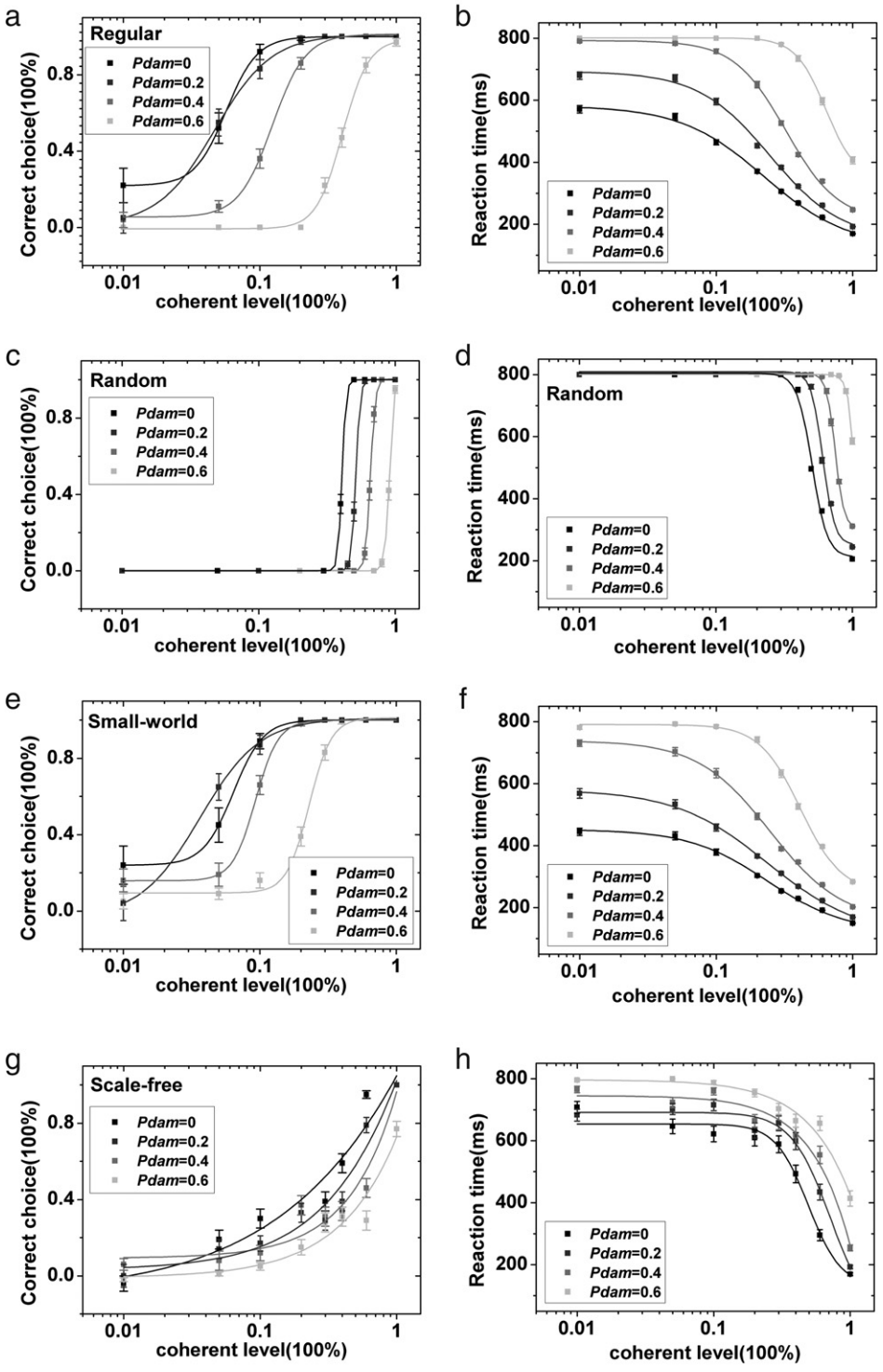

Fig. 9. Effects of network topology on decision-making performance subject to distributed neuronal damage. a. The regular network shows severe decrease of accuracy in decision-making, especially in the high distributed damage ($P_{\text{dam}} = 0.4, 0.6$). b. The regular network shows a gradual increase in reaction time with an increase of P_{dam}. c, d. The random network shows a gradual decrease in performance, in terms of both accuracy and reaction time with an increase of P_{dam}. e, f. The small-world network also shows decreased accuracy and increased reaction time with an increase of P_{dam}. g, h. The scale-free network shows a gradual decrease in both accuracy and reaction time with an increase of P_{dam}. Data are fitted by the logistic curve ($R^2 > 0.99$ for all curves in a–f; $R^2 > 0.94$ for all curves in g, h). For each test point, the data are obtained after an average of 100 trials. The error bar indicates the SEM.

In this case, the short path length in the small-world network facilitates the spread of the competing signals to the inactivated neurons, which leads to a larger recruitment cluster, compared with the recruitment in the regular network. Therefore, the small-world network shows the shortest reaction time among the three networks. Taken together, different network topologies contribute to certain network behaviors under different conditions.

Besides the small-world network, the scale-free network is also becoming a research hotspot in the field of complex networks, which has been identified in many biological and other systems

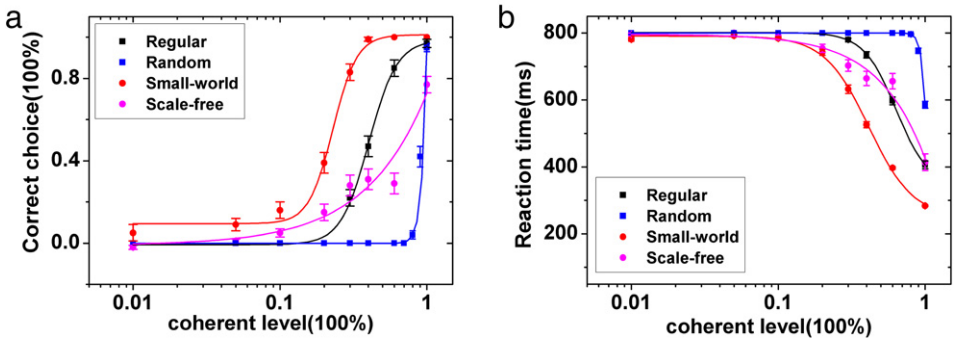

Fig. 10. Comparison of network behaviors at the distributed damage P_{dam} of 0.6. The small-world network displays the best performance in terms of both accuracy (a) and reaction time (b) among all networks. The decision-making process is simulated in the low internal noise situation ($\sigma = 0.5$). Data are fitted by the logistic curve ($R^2 > 0.99$ for black, blue, and red curves; $R^2 = 0.94$ and $R^2 = 0.97$ for magenta curves in a and b respectively). For each test point, the data are obtained after an average of 100 trials. The error bar indicates the SEM. (For interpretation of the references to colour in this figure legend, the reader is referred to the web version of this article.)

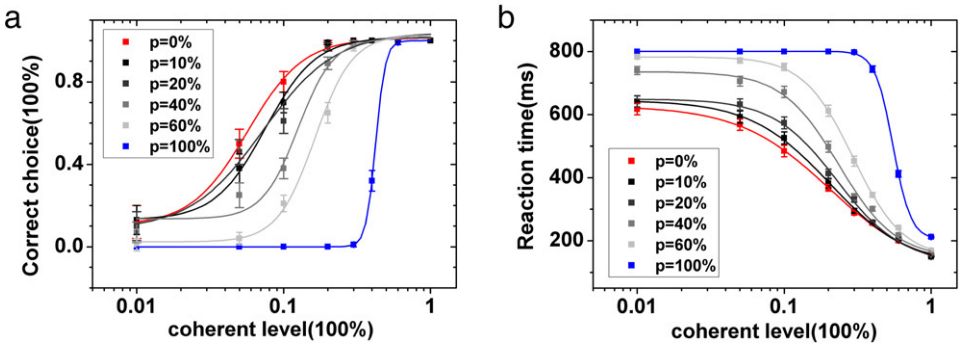

Fig. 11. Effects of network topologies on network behaviors in the small-world network. During the construction of the small-world network, the percentages of the random connections systematically varied from 0% to 100%. Following the increase of the random components, the networks show a gradual decrease in both accuracy (a) and reaction time (b). Specifically, the networks with small random connections ($p = 10\%$, $p = 20\%$) show a similar decision-making process to the regular network, especially in terms of accuracy. The modified parameters are: $N = 200$, $\varepsilon = 0.1$. Data are fitted by the logistic curve ($R^2 > 0.98$ for all curves). For each test point, the data are obtained after an average of 100 trials. The error bar indicates the SEM.

(Albert & Barabasi, 2002). However, in the present study the scale-free network only shows a medium performance. From the topological view, the scale-free network has a small clustering coefficient, which may result in poor performance in decision-making. From the biological point of view, we also believe its medium performance to be reasonable. The neural groups we constructed are used to mimic a particular brain structure that contributes to the decision-making process. In the brain structure, there is no biological evidence to support the assumption that a few neurons "own" a large proportion of synaptic connections. Instead, most of neurons inside the brain structure (such as cortical pyramidal cells) should be homogenous in terms of connection probability. Otherwise, the removal of some "essential" neurons (in the case of neurodegeneration or neural injury) may result in fatal damage to the whole brain structure. However, the existence of these "essential" nodes is one of the basic properties of the scale-free network. In addition, recent evidence demonstrates that the formation of some brain structure, such as the brainstem reticular formation, is a small-world, but not scale-free, network (Humphries, Gurney, & Prescott, 2006). Although further study is required to determine whether the brain areas such as the parietal regions, which contribute to the decision-making process in animals, also have this small-world, but not scale-free properties, our results might offer some helpful insights into this aspect of the computational principle.

Taken together, different network topologies have some advantages under different conditions. Overall, the small-world network retains a good overall network behavior in many cases. Our findings indicate that the network topology is an essential factor for consideration when constructing neural networks. In particular, the relatively better overall performance of small-world networks begs the question of whether biological decision-making networks actually have this particular network topology. Finally, our computational modeling results contribute to a better understanding between neuronal connections and cognition such as decision-making.

Acknowledgements

We thank Liang Chen, Zhihua Wu, and Si Wu for critical reading of the manuscript. We also thank the reviewers/referees for their constructive suggestions during the revision of the manuscript.

References

Albert, R., & Barabasi, A. L. (2002). Statistical mechanics of complex networks. *Reviews of Modern Physics*, *74*, 47–97.
Albert, R., Jeong, H., & Barabasi, A. L. (2000). Error and attack tolerance of complex networks. *Nature*, *406*, 378–382.
Amit, D. J., & Brunel, N. (1997). Model of global spontaneous activity and local structured activity during delay periods in the cerebral cortex. *Cerebral Cortex*, *7*, 237–252.
Barabasi, A. L., & Albert, R. (1999). Emergence of scaling in random networks. *Science*, *286*, 509–512.
Boccaletti, S., Latora, V., Moreno, Y., Chavez, M., & Hwang, D. U. (2006). Complex networks: Structure and dynamics. *Physics Report*, *424*, 175–308.
Bogacz, R. (2007). Optimal decision-making theories: Linking neurobiology with behaviour. *Trends in Cognnatiue Sciences*, *11*, 118–125.
Bogacz, R., Brown, E., Moehlis, J., Holmes, P., & Cohen, J. D. (2006). The physics of optimal decision making: A formal analysis of models of performance in two-alternative forced-choice tasks. *Psychological Review*, *113*, 700–765.
Britten, K. H., Shadlen, M. N., Newsome, W. T., & Movshon, J. A. (1993). Responses of neurons in macaque MT to stochastic motion signals. *Visual Neuroscience*, *10*, 1157–1169.

Ditterich, J. (2006). Evidence for time-variant decision making. *European Journal of Neuroscience*, *24*, 3628–3641.
Durstewitz, D., Seamans, J. K., & Sejnowski, T. J. (2000). Neurocomputational models of working memory. *Natural Neuroscience*, *3*(Suppl), 1184–1191.
Ganguli, S., Bisley, J. W., Roitman, J. D., Shadlen, M. N., Goldberg, M. E., & Miller, K. D. (2008). One-dimensional dynamics of attention and decision making in LIP. *Neuron*, *58*, 15–25.
Glimcher, P. W. (2003). The neurobiology of visual-saccadic decision making. *Annual Review of Neuroscience*, *26*, 133–179.
Humphries, M. D., Gurney, K., & Prescott, T. J. (2006). The brainstem reticular formation is a small-world, not scale-free, network. *Proceedings of the Royal Society of London. Series B-Biological Sciences*, *273*, 503–511.
Machens, C. K., Romo, R., & Brody, C. D. (2005). Flexible control of mutual inhibition: A neural model of two-interval discrimination. *Science*, *307*, 1121–1124.
Mazurek, M. E., Roitman, J. D., Ditterich, J., & Shadlen, M. N. (2003). A role for neural integrators in perceptual decision making. *Cerebral Cortex*, *13*, 1257–1269.
Newman, M. E. J. (2003). The structure and function of complex networks. *SIAM Review*, *45*, 167–256.
Newsome, W. T., Britten, K. H., & Movshon, J. A. (1989). Neuronal correlates of a perceptual decision. *Nature*, *341*, 52–54.
Parker, A. J., & Newsome, W. T. (1998). Sense and the single neuron: Probing the physiology of perception. *Annual Review of Neuroscience*, *21*, 227–277.
Platt, M. L. (2002). Neural correlates of decisions. *Current Opinion Neurobiology*, *12*, 141–148.
Roitman, J. D., & Shadlen, M. N. (2002). Response of neurons in the lateral intraparietal area during a combined visual discrimination reaction time task. *Journal of Neuroscience*, *22*, 9475–9489.
Romo, R., & Salinas, E. (2001). Touch and go: Decision-making mechanisms in somatosensation. *Annual Review of Neuroscience*, *24*, 107–137.
Romo, R., & Salinas, E. (2003). Flutter discrimination: Neural codes, perception, memory and decision making. *Nature Review Neuroscience*, *4*, 203–218.
Schall, J. D. (2001). Neural basis of deciding, choosing and acting. *Natural Review Neuroscience*, *2*, 33–42.
Shadlen, M. N., & Newsome, W. T. (1996). Motion perception: Seeing and deciding. *Proceedings of the National Academy of Sciences of the USA*, *93*, 628–633.
Shadlen, M. N., & Newsome, W. T. (2001). Neural basis of a perceptual decision in the parietal cortex (area LIP) of the rhesus monkey. *Journal of Neurophysiology*, *86*, 1916–1936.
Smith, P. L., & Ratcliff, R. (2004). Psychology and neurobiology of simple decisions. *Trends in Neurosciences*, *27*, 161–168.
Sugrue, L. P., Corrado, G. S., & Newsome, W. T. (2005). Choosing the greater of two goods: Neural currencies for valuation and decision making. *Nature Review Neuroscience*, *6*, 363–375.
Usher, M., & McClelland, J. L. (2001). The time course of perceptual choice: The leaky, competing accumulator model. *Psychological Review*, *108*, 550–592.
Wang, X. J. (2002). Probabilistic decision making by slow reverberation in cortical circuits. *Neuron*, *36*, 955–968.
Watts, D. J., & Strogatz, S. H. (1998). Collective dynamics of 'small-world' networks. *Nature*, *393*, 440–442.
Wong, K. F., & Wang, X. J. (2006). A recurrent network mechanism of time integration in perceptual decisions. *Journal of Neuroscience*, *26*, 1314–1328.